Tapered silicon optical fibers

N. Healy[1], J. R. Sparks[2], P. J. A. Sazio[1], J. V. Badding[2], and A. C. Peacock[1]*

[1] *Optoelectronics Research Centre, University of Southampton, Southampton SO17 1BJ, UK*
[2] *Department of Chemistry and Materials Research Institute, Pennsylvania State University, 16802 PA, USA*

**acp@orc.soton.ac.uk*

Abstract: The tapering of silicon optical fibers is demonstrated using a fusion splicer. The silicon fibers are fabricated using a high pressure chemical deposition technique to deposit an amorphous silicon core inside a silica capillary and the tapering is performed in a separate post-process. Optical and material characterization has revealed a smooth transition region leading to a uniform tapered waist that are both simultaneously crystallized to yield a solid polysilicon core. The strong mode confinement and low taper loss measured in the silicon fibers verifies this tapering approach for the fabrication of structures with nanoscale core dimensions.

OCIS codes: (060.2280) Fiber design and fabrication; (060.2290) Fiber materials; (190.4370) Nonlinear optics, fibers; (160.6000) Semiconductor materials.

References and links

1. A. C. Turner, C. Manolatou, B. S. Schmidt, M. Lipson, M. A. Foster, J. E. Sharping, and A. L. Gaeta, "Tailored anomalous group-velocity dispersion in silicon channel waveguides," Opt. Express **14**, 4357–4362 (2006).
2. V. R. Almeida, R. R. Panepucci, and M. Lipson, "Nanotaper for compact mode conversion," Opt. Lett. **28**, 1302–1304 (2003).
3. M. Krause, H. Renner, and E. Brinkmeyer, "Efficient Raman Lasing in Tapered Silicon Waveguides," Spectroscopy **21**, 26 (2006).
4. A. Kudlinski, A. K. George, J. C. Knight, J. C. Travers, A. B. Rulkov, S. V. Popov, and J. R. Taylor, "Zero-dispersion wavelength decreasing photonic crystal fibers for ultraviolet-extended supercontinuum generation," Opt. Express **14**, 5715–5722 (2006).
5. M. Lipson, "Overcoming the limitations of microelectronics using Si nanophotonics: solving the coupling, modulation and switching challenges," Nanotechnology **15**, S622–S627 (2004).
6. B. Jalali and S. Fathpour, "Silicon Photonics," J. Lightwave Technol. **24**, 4600–4615 (2006).
7. P. J. A. Sazio, A. Amezcua-Correa, C. E. Finlayson, J. R. Hayes, T. J. Scheidemantel, N. F. Baril, B. R. Jackson, D.-J. Won, F. Zhang, E. R. Margine, V. Gopalan, V. H. Crespi, and J. V. Badding, "Microstructured Optical Fibers as High-Pressure Microfluidic Reactors," Science **311**, 1583–1586 (2006).
8. J. Ballato, T. Hawkins, P. Foy, R. Stolen, B. Kokuoz, M. Ellison, C. McMillen, J. Reppert, A. M. Rao, M. Daw, S. Sharma, R. Shori, O. Stafsudd, R. R. Rice, and D. R. Powers, "Silicon optical fiber," Opt. Express **16**, 18675–18683 (2008).
9. B. Scott, K. Wang, V. Caluori, and G. Pickrell, "Fabrication of silicon optical fiber," Opt. Eng. **48**, 100501 (2009).
10. C. R. Kurkjian, J. T. Krause, and M. J. Matthewson, "Strength and Fatigue of Silica Optical Fibers," J. Ligthwave Technol. **7**, 1360–1370 (1989).
11. P. J. Roberts, F. Couny, H. Sabert, B. J. Mangan, D. P. Williams, L. Farr, M. W. Mason, A. Tomlinson, T. A. Birks, J. C. Knight, and P. St. J. Russell, "Ultimate low loss of hollow-core photonic crystal fibres," Opt. Express **13**, 236–244 (2005).
12. L. Lagonigro, N. V. Healy, J. R. Sparks, N. F. Baril, P. J. A. sazio, J. V. Badding and A. C. Peacock, "Wavelength-dependent loss measurements in polysilicon modified optical fibres," CLEO/Europe-EQEC **CE3** (2009).
13. K. H. Guenther, P. G. Wierer, and J. M. Bennett, "Surface roughness measurements of low-scatter mirrors and roughness standards," Appl. Opt. **23**, 3820–3836 (1984).
14. L. Lagonigro, N. Healy, J. R. Sparks, N. F. Baril, P. J. A. Sazio, J. V. Badding, and A. C. Peacock, "Low loss silicon fibers for photonics applications," Appl. Phys. Lett. **96**, 041105 (2010).

#122659 - $15.00 USD Received 12 Jan 2010; revised 25 Feb 2010; accepted 26 Feb 2010; published 29 Mar 2010

15. N. Healy, J. R. Sparks, M. N. Petrovich, P. J. A. Sazio, J. V. Badding, and A. C. Peacock, "Large mode area silicon microstructured fiber with robust dual mode guidance," Opt. Express **17**, 18076–18082 (2009).
16. M. J. A. de Dood, A. Polman, T. Zijlstra, and E. W. J. M. van der Drift, "Amorphous silicon waveguides for microphotonics," J. Appl. Phys. **92**, 649–653 (2009).

1. Introduction

Micro and nanoscale waveguides have played an integral role in the recent success of silicon photonics forming the basis of a number of compact optoelectronic devices. The high refractive index of the silicon core allows for strong mode confinement in the subwavelength structures to enhance the nonlinear interactions and tune the waveguide dispersion [1]. An interesting extension which allows for the continuous tailoring of the nonlinear and dispersion effects is to taper the silicon waveguides. To date, silicon tapers have primarily been used to improve the coupling efficiency between micron sized silica fibers and nanoscale silicon waveguides by reducing reflection losses and mode mismatch [2]. However, like their more conventional tapered silica fiber counterparts, silicon tapers could also find use in applications which require longitudinally varying waveguide properties, for example, in highly efficient Raman amplification [3] and extended broadband supercontinuum generation [4].

Although most silicon devices are based on lithographically defined single crystal silicon-on-insulator (SOI) waveguides [5, 6], recently there has been an increased interest in a new class of waveguide, the silicon optical fiber [7–9]. Typically, these fibers are fabricated by filling a silica capillary with the semiconductor material making them analogous to the SOI waveguides. Importantly, however, the fiber template offers some unique properties in that it provides an extremely smooth deposition surface, it has a cylindrically symmetric geometry, reducing polarization sensitivity, it is robust, flexible, and can be fabricated with a range of transverse dimensions. Further to this, fiber templates can easily be post-processed via tapering which is a well established method of obtaining an additional degree of control over the waveguiding characteristics, and also allows for the convenient fabrication of nanoscale waveguides from micron sized starting dimensions.

In this paper we investigate the potential to taper silicon fibers using a fusion splicer. The silicon fibers are fabricated using a high pressure microfluidic chemical deposition technique to completely fill the capillary pore with amorphous material over lengths of several centimeters [7]. We consider the tapering of silicon fibers with a range of core sizes to establish the capabilities of this technique. Optical microscopy and Raman measurements are used to monitor the quality of the semiconductor material in the tapered region. The low loss induced by tapering the silicon fibers demonstrates their potential to be exploited in a wide range of applications that require a controlled variation in the waveguide's modal and propagation properties.

2. Fabrication and Materials Characterization

Infiltration of bulk silicon into the hole of the capillary template to create the fiber structure is conducted using a high pressure microfluidic chemical deposition technique [7], possible due to the excellent mechanical strength of silica [10]. Silica capillaries are particularly well suited for use as templates for the deposition of high index materials as they have extremely smooth internal surfaces (0.1 nm root mean square roughness [11]). This results in minimal roughness at the core-cladding interface to reduce surface scattering, which is one of the major contributors to transmission losses in nanoscale waveguides. The deposition process is conducted by forcing a mixture of silane and helium (SiH_4/He) to flow through the central hole under high pressures ~ 35 MPa and temperatures that range between $350-500\,^{\circ}$C. By limiting the process temperature to be below $500\,^{\circ}$C we ensure that the material deposits in an amorphous state so that it bonds smoothly to the silica walls [12].

#122659 - $15.00 USD Received 12 Jan 2010; revised 25 Feb 2010; accepted 26 Feb 2010; published 29 Mar 2010

To demonstrate the versatility of this tapering technique, we taper three silicon fibers with external silica capillary diameters in the range $110-160\,\mu$m but with different starting core diameters of $5.6\,\mu$m, $2.7\,\mu$m and $1.3\,\mu$m. The fibers were tapered using a BIT communications BFF-60 arc fusion splicer. The arc current was chosen to be in the range $8-15\,$mA, set for a duration of $5.5\,$s, to ensure that the silicon was above its melting point of $1410\,^{\circ}$C, and the pull distance was selected so that the fibers' taper ratios were of the order $1:2$. Fig. 1 shows microscope images of the resulting tapered fibers where (a) is the $5.6\,\mu$m fiber tapered to a core waist of $\sim 3\,\mu$m, (b) is the $2.7\,\mu$m fiber tapered to $\sim 1\,\mu$m and (c) is the $1.3\,\mu$m fiber tapered to $\sim 500\,$nm. These images show that the tapering process has produced a solid, defect free, silicon core with a smooth transition from the untapered fiber to the taper waist, where at each point along the taper the core diameter changes proportionally to the changing cladding diameter. In all cases the total taper length is $\sim 700\,\mu$m, with a waist of $\sim 100\,\mu$m, so that the taper angle is large. Although such strong tapers are usually undesirable in standard single mode fiber tapers as they lead to excessive coupling to radiation modes, this is not the case in silicon tapers, at least for the lower order modes, because of the large core-cladding index contrast [2].

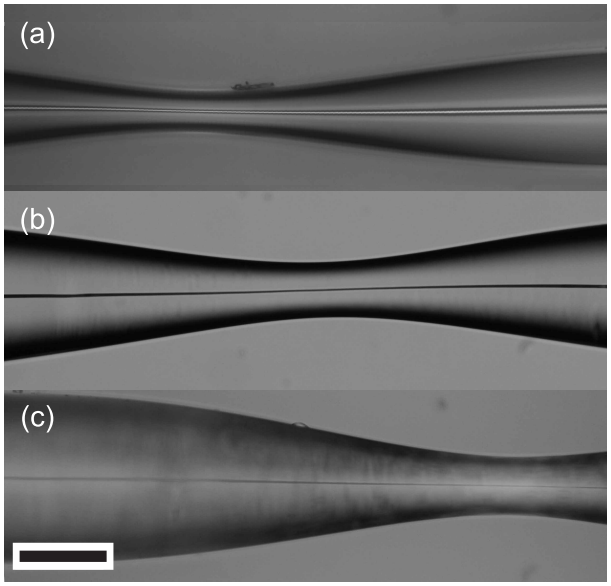

Fig. 1. Brightfield microscope images (diascopic illumination) of the longitudinal taper profiles for starting fiber core diameters of (a) $5.6\,\mu$m, (b) $2.7\,\mu$m, and $1.3\,\mu$m. The $70\,\mu$m scale bar is applicable for all images.

To investigate the surface roughness at the core-cladding interface, differential interference contrast (DIC) microscopy images of the $2.7\,\mu$m fiber were collected with a $100\times$ oil immersion objective lens over the length of the tapered region, as shown in Fig. 2(a). DIC, as an interferometric technique, under ideal circumstances, is sensitive to height differences as small as $0.2\,$nm and can easily detect $1\,$nm differences [13]. The lack of image contrast indicates that the surface roughness is less than $1\,$nm. We note that the complete void-free filling of the capillary with amorphous silicon during the initial deposition is critical to the success of the tapering process. It is for this reason that the silicon fibers maintain their very smooth, void-free silica-silicon interface upon melting, thus demonstrating the advantage of this tapering approach for the fabrication of nanoscale waveguides.

The material quality of the silicon was then determined via micro-Raman measurements over

#122659 - $15.00 USD Received 12 Jan 2010; revised 25 Feb 2010; accepted 26 Feb 2010; published 29 Mar 2010

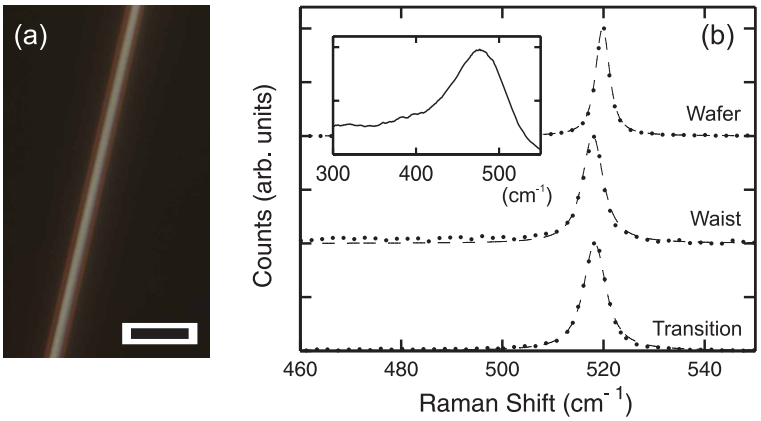

Fig. 2. (a) DIC image of the 2.7 μm fiber taper; scale bar 3 μm. (b) Micro-Raman spectra for three positions along the 2.7 μm fiber core: untapered region (inset), taper transition (bottom), taper waist (middle) and a single crystal silicon wafer (top). Dashed lines are Voigt fits including Gaussian instrument broadening of 2.1 cm^{-1}.

the tapered region. At each point a 633 nm HeNe laser was focused onto the silicon through the side of the transparent silica cladding, with a spot size of $\sim 2\,\mu$m and ~ 3 mW of power at the outer surface, and the backscattered radiation recorded on a thermoelectrically cooled Horiba Jobin Yvon Synapse CCD detector. Figure 2(b) shows the measured Raman spectra taken at three positions along the 2.5 μm fiber: the untapered fiber (inset), the taper transition (bottom curve), and the taper waist (middle curve), together with a reference spectrum taken of a single crystal silicon wafer (top curve). From these spectra it is clear that whilst the untapered fiber has retained the amorphous silicon nature, evident from the broad peak around 480 cm^{-1}, both the taper transition and the waist have a narrow peak at 518 cm^{-1} revealing that the silicon core has crystallized during the tapering. This crystallization is not unexpected and is due to the melting and subsequent solidification that the silicon core experiences during tapering. To establish the quality of the polysilicon material in the taper region we have fitted the Raman spectra with Voigt profiles (dashed curves) to account for the 2.1 cm^{-1} Gaussian instrument contribution to the Lorentzian peak width. The silicon wafer has a Lorentzian full width at half maximum (FWHM) of 2.7 cm^{-1}, centered at 520 cm^{-1}, with the polysilicon widths measured to be 4.6 cm^{-1} at the taper transition and 4.3 cm^{-1} at the taper waist, which are comparable to Raman peak widths measured in other polysilicon fibers [14, 15]. The broadening, and asymmetry of the tapered peaks, when compared to the reference spectrum, are due to contributions from defect and amorphous materials that surround the single crystal grains. We attribute the smaller width at the taper waist to a larger reduction in the defect and amorphous content, which is likely to be due to a faster cooling rate in this region. Further improvement to the material quality should be possible by annealing the entire fiber which will crystallize the untapered amorphous material and reduce the defect material in the tapered region [14, 15]. We note that similar characterization conducted on the 5.6 μm and 1.3 μm tapered fibers has yielded comparable results.

3. Optical Transmission Properties

To determine the longitudinally varying dispersion and nonlinear waveguiding properties of these silicon fiber tapers we have conducted modal simulations using a full vector finite element method (FEM). Although the precise values of the refractive index of the deposited, and

#122659 - $15.00 USD Received 12 Jan 2010; revised 25 Feb 2010; accepted 26 Feb 2010; published 29 Mar 2010

crystallized, silicon material are not known, we can still obtain qualitative information about the tapers' properties by approximating the index with that of single crystal silicon. Figure 3 shows the effective fundamental mode (a) index and (b) area for silicon core diameters over the range 500 nm – 2.5 μm, for a transmission wavelength of 1550 nm. From these curves it is evident that for micron sized core diameters, there is only a moderate change in the effective mode index as the diameter is reduced, and a corresponding decrease in the mode area associated with the mode remaining confined to the core. However, as the core size enters the nanoscale regime, the mode starts to interact more strongly with the silica cladding resulting in a more dramatic decrease in the effective index and a less pronounced decrease in the area as the diameter is further reduced. The group velocity dispersion (GVD) parameter is then shown in Fig. 3(c). Although crystalline silicon has a large normal material dispersion, it is well known that waveguide dispersion dominates as the core size is reduced [1], and for core diameters less than $\sim$ 925 nm we expect the dispersion in the tapers to be anomalous. Thus by using this tapering technique we can fabricate silicon waveguides with varying effective dispersion profiles that can seamlessly link between the normal and anomalous regimes.

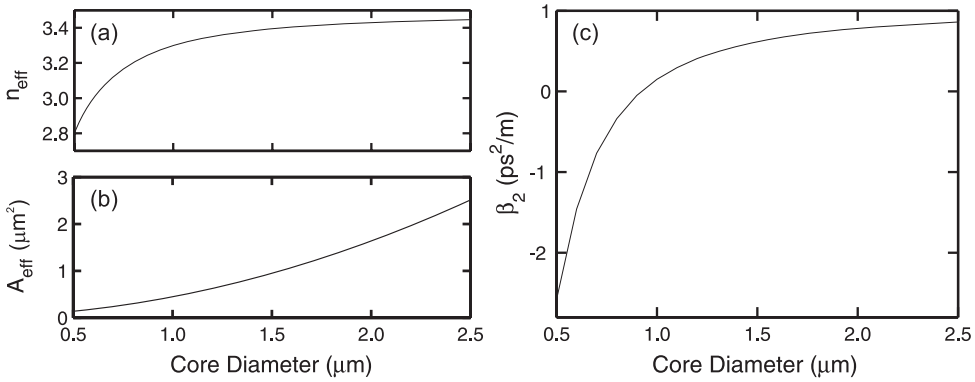

Fig. 3. Effective fundamental mode (a) index and (b) area as functions of the taper core diameter, together with the corresponding (c) group velocity dispersion parameter. All calculations are for a transmission wavelength of 1550 nm.

The waveguiding properties of the silicon fiber tapers were established by measuring the transmission of a 0.5 mW continuous wave 1550 nm diode. Efficient coupling into and out of the tapers is ensured by preparing the end faces by first mounting them inside a thicker capillary tube and then using a standard polishing technique. Figure 4 shows optical microscope images of the polished cross sections of the 2.7 μm tapered fiber corresponding to the three regions: (a) untapered fiber, (b) taper transition (core size 1.9 μm) and (c) taper waist (core size 1.2 μm), from which it is evident that the core and cladding have retained their circular shape and that the tapering process has reduced their diameters by the same ratio. The light is launched into the untapered end of a 2 mm long structure using a 40$\times$ microscope objective lens and a second 25$\times$ objective is used to capture the transmitted light and focus it onto an Electrophysics infrared camera. The bottom images in Fig. 4 show the near field modes exiting the three core sizes displayed above, where it is evident that the light is well confined to the core. Unfortunately, due to the untapered amorphous silicon section of the fiber, which has a high transmission loss associated with dangling bond absorption [16], the total device loss is large ($\sim$ 12 dB). However, we have previously determined that the losses in silicon fibers can be dramatically improved via optimization of the starting amorphous material and the annealing conditions [14], and thus we anticipate that a similar approach can be applied here. Significantly, by using a replacement method where we compare the loss in the tapered fiber with an

#122659 - $15.00 USD Received 12 Jan 2010; revised 25 Feb 2010; accepted 26 Feb 2010; published 29 Mar 2010

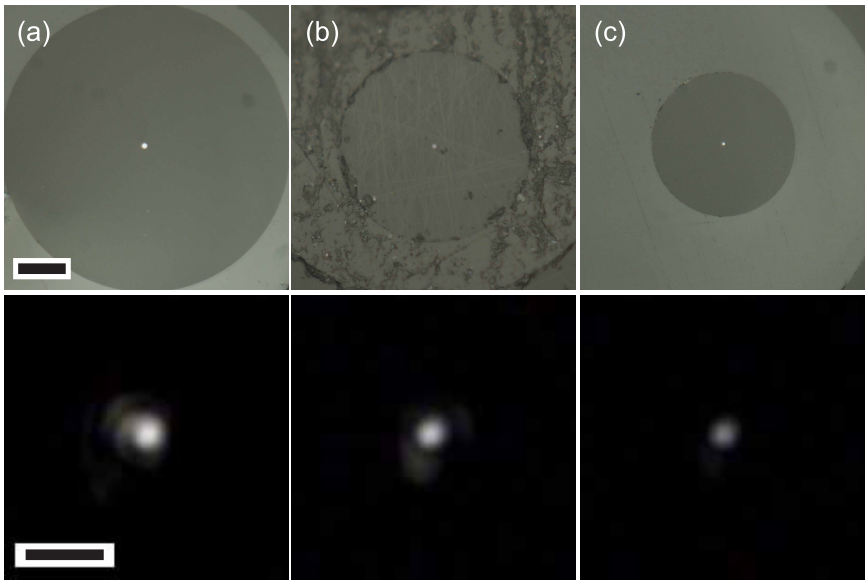

Fig. 4. Top: microscope images of the polished cross sections of the 2.7 μm tapered fiber corresponding to the three regions: (a) untapered fiber (scale bar 30 μm), (b) taper transition and (c) taper waist, all at the same scale . Bottom: near field mode profiles exiting the three core sizes displayed above, all imaged at the same scale (scale bar 4 μm).

untapered fiber of the same length and material composition, we estimate a taper loss of only ~ 0.5 dB. This loss is most likely due to the fact that the taper has a non-adiabatic transition for the higher order modes, and thus we expect that it could be reduced by lengthening the taper transition or limiting the number of modes supported by the starting silicon fiber [15]. Nevertheless, the strong mode confinement and the extremely smooth core-cladding interface in the silicon fiber tapers verifies this approach for the fabrication of structures with nanoscale core dimensions.

4. Conclusion

We have demonstrated the fabrication of silicon fiber tapers using a fusion splicer. Optical and material characterization has revealed a smooth transition region and a uniform core waist that are both simultaneously crystallized to polysilicon. Tapered waveguides are useful both for improving the coupling efficiency between structures with differing core indices, and for tailoring the nonlinear and dispersion properties. In particular, control of the size and sign of the effective dispersion is critical not only for dispersion compensation schemes but also for improving phase-matching conditions, and thus efficiencies, of a number of nonlinear processes. The strong mode confinement and low optical losses measured in the silicon fiber tapers verifies this approach for the fabrication of nanoscale structures. Owing to the ease and versatility of this technique we expect silicon fiber tapers to find wide ranging applications in the next generation of silicon photonics devices.

Acknowledgments

The authors acknowledge EPSRC (EP/G028273/1), NSF (DMR-0806860) and the Penn State Materials Research Science and Engineering Center (NSF DMR-0820404) for financial support. A. C. Peacock is a holder of a Royal Academy of Engineering fellowship.

#122659 - $15.00 USD Received 12 Jan 2010; revised 25 Feb 2010; accepted 26 Feb 2010; published 29 Mar 2010